A Joint Experimental/Computational Investigation of the Structural and Spectroscopic Properties of PVDF Polymorphs.

ARTICLE *in* THE JOURNAL OF PHYSICAL CHEMISTRY B · MARCH 2015

Impact Factor: 3.3 · DOI: 10.1021/acs.jpcb.5b00161 · Source: PubMed

3 AUTHORS, INCLUDING:

Alberto Milani

Politecnico di Milano

59 PUBLICATIONS **467** CITATIONS

SEE PROFILE

Stefano Radice

Solvay

32 PUBLICATIONS **391** CITATIONS

SEE PROFILE

THE JOURNAL OF PHYSICAL CHEMISTRY B

Article

pubs.acs.org/JPCB

Joint Experimental and Computational Investigation of the Structural and Spectroscopic Properties of Poly(vinylidene fluoride) Polymorphs

Alberto Milani,*[,†] Chiara Castiglioni,[†] and Stefano Radice[‡]

[†]Politecnico di Milano, Dip. Chimica, Materiali, Ing. Chimica "G. Natta" P.zza Leonardo da Vinci 32, 20133 Milan, Milano, Italy

[‡]Solvay Specialty Polymers RD&T Center, Viale Lombardia 20, 20021 Bollate, Milano, Italy

Supporting Information

ABSTRACT: State-of-the-art density functional theory calculations are here adopted for the investigation of the crystal structure and of the vibrational properties of α, β, γ, and δ phases of poly(vinylidene fluoride) (PVDF), in comparison with IR and Raman measurements. DFT calculations allowed a detailed interpretation of the IR and Raman spectra of α and β phases, giving vibrational assignments useful for qualitative and quantitative characterization of these systems. From a molecular perspective, the computational investigation of the crystal structure and the spectra of PVDF polymorphs helped in clarifying the role of supramolecular dipole−dipole interactions, which indeed modulate the vibrational properties of these systems, indicating also that intermolecular interaction could play a significant role in the modulation of ferroelectric properties. Furthermore, the combined experimental and computational approach allowed us to identify and characterize the thermally and mechanically induced γ phase, shedding light on the far-IR marker bands of this elusive phase of PVDF.

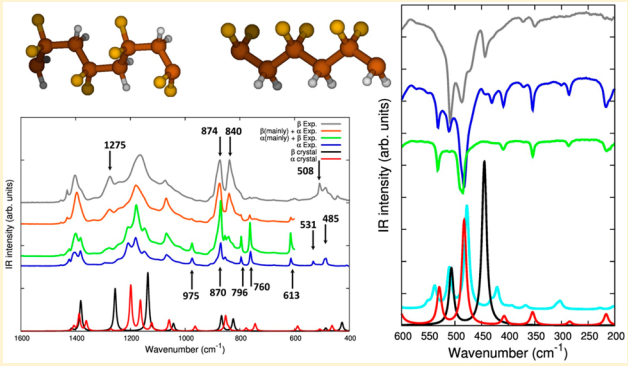

1. INTRODUCTION

Since the discovery of the piezoelectric properties of poly(vinylidene fluoride) (PVDF),[1] this polymer attracted the attention of many research groups dealing with both fundamental and applied studies, generating an impressive amount of investigations and well-assessed technological applications in several different fields.[2−7] Due to the molecular nature of this material, the interplay between intra- and intermolecular effects and the supramolecular organization of the PVDF molecules in the solid state play a major role in determining its ferroelectric properties. PVDF in particular presents a quite complex behavior, due to the existence of four different crystal polymorphs, displaying different electrical activity. PVDF preferentially crystallizes in the nonpolar α phase (form II, TGTG′ conformation), which can be converted by stretching and poling to the polar β phase (form I, all-trans conformation) where the ferroelectric response of the materials is maximized. In addition to these two main phases, two other polar phases, γ (form III, T_3GT_3G') and δ (form IV or polar α, TGTG′ conformation), can be generated but received less attention due to their much more elusive character and the lower ferroelectric response with respect to β-PVDF. Several different investigations aimed at the determination of the chain conformation and crystal structure of PVDF polymorphs have been presented in the past and still receive particular attention by the scientific community.[8−15] In this context, a significant example is the very recent paper by Li et al.[15] where the crystal structure of δ-PVDF is revisited in connection with the discovery of new interesting preparation methods and also with the perspective of possible new applications for this polymorph. The importance of a detailed understanding of the structural features of PVDF polymorphs is not limited to the homopolymer itself but extends also to its copolymers with tri- and tetrafluoroethylene, which found an even wider fortune for technological applications due to the easiest formation of a large amount of ferroelectric β phase thanks to copolymerization.[5,6] Furthermore, new systems (such as terpolymers with chlorofluoroethylene blocks[16]) have been investigated, to tune and further improve the electrical response of these materials from both a chemical and a structural perspective. In these cases, apart from X-ray diffraction experiments, vibrational spectroscopy played an important role for the characterization of PVDF and PVDF-based systems.[17−27] Moreover, the predictive power of state-of-the-art first-principles calculations enabled support of the experimental measurements by means of accurate modeling, concerning the structural determination, the spectroscopic analysis, and the calculation of the polarization properties.[25−35] Considering in particular the vibrational

Received: January 7, 2015
Revised: March 13, 2015
Published: March 16, 2015

DOI: 10.1021/acs.jpcb.5b00161
J. Phys. Chem. B 2015, 119, 4888−4897

properties of PVDF, investigation of which is the main focus of this paper, a few computational studies based on density functional theory have been presented in the recent literature reporting the prediction of the vibrational frequencies of α and β polymorphs in particular.[25−27] Very recently, Itoh et al. extended the computational analysis also to γ and δ phases, including the prediction of the static polarization properties.[35] However, in none of these works has a comparison in frequency and intensity pattern between experimental and computed spectra been presented, thus limiting the potential information that can be obtained by a combined experimental and computational approach. The scope of our paper is to provide a detailed and thorough interpretation of the experimental IR and Raman spectra of PVDF polymorphs by means of state-of-the-art quantum chemical approaches of solid state chemistry, aiming at obtaining new insights on the structural phenomena involved at the nanoscale. In this way, we will obtain a reliable assignment of the spectra also in their minor features, which would serve for practical applications in more general contexts. To this aim, periodic (periodic boundary conditions) density functional theory calculations will be carried out by means of the CRYSTAL14[36−39] software, as also proposed in ref 35, and theoretical predictions will be compared with experimental measurements. Indeed, this code proved to be particularly reliable for the detailed prediction of the structure and the vibrational properties of crystalline polymers,[40−49] providing a powerful tool to shed light on subtle polymorphic effects[43,46,48] or to carry out a detailed assignment of the vibrational spectra,[40,41,44,47] including other fluorinated polymers.[45]

In Section 3, the results obtained by means of this joint experimental and computational approach will be presented: we will first test the reliability of different computational setups based on their ability to reproduce the experimental crystal structure of the different polymorphs; on this basis the IR and Raman spectra will be predicted and the experimentally observed transitions will be assigned, thus allowing new interpretations based on the thermal/mechanical evolution of the IR response. The results confirm that PVDF polymorphs still present phenomena and properties that require a deep investigation and demonstrate that only by joining the experimental and theoretical perspectives is it possible to give accurate and reliable interpretations.

2. MATERIALS AND METHODS

2.1. Computational Details. Full geometry optimization of the crystal structure and chain conformation and the prediction of the IR and Raman spectra of α, β, γ, and δ polymorphs of PVDF have been carried out by means of the CRYSTAL14 code[36−39] in the framework of density functional theory. In order to test the accuracy of different combinations of DFT functionals and basis sets, the crystal structure optimization has been carried out employing both the B3LYP[50,51] and PBE0[52] hybrid exchange-correlation functionals, combined with 6-31G(d,p) and the recently developed pob-TZVP[53] basis set. Based on previous computational investigations of polymer systems,[43−49] we introduced the empirical correction for dispersion interaction (DFT-D) proposed by Grimme[54−56] (related parameters are taken from ref 43), since it has been demonstrated that it can be very beneficial for a reliable description of both the structure and the vibrational spectra. However, in light of the results reported in a previous investigation,[35] crystal geometry optimizations have been carried out also at B3LYP/pob-TZVP and PBE0/pob-TZVP level without correction for dispersion interactions.

In all calculations, the atomic positions and the lattice parameters were fully optimized. As first guess input structures, the experimentally determined structures have been adopted: for α-PVDF we used the data reported by Hasegawa et al.[8] and Li et al.,[15] for β-PVDF those reported by Hasegawa et al.,[8] and for γ-PVDF we adopted the same experimental input geometry reported by Itoh et al.,[35] while for δ-PVDF data have been taken from Li et al.[15]

In addition to the simulations of the crystals, we carried out also simulations for infinite one-dimensional polymer chains (1D crystal), considering as starting geometries the structures showing the conformations observed in α- (and δ-), β-, and γ-PVDF crystals and imposing periodic boundary conditions in chain axis direction. The optimized structures of these 1D model chains and of the chain packing in β-PVDF crystal are sketched in Figure 1.

In all cases, normal frequencies calculation at Γ point have been carried out on the optimized geometries as achieved by diagonalization of the (numerically calculated) Hessian matrix.

The DFT computed spectra have been compared with the experimental ones. As usual when carrying out such a

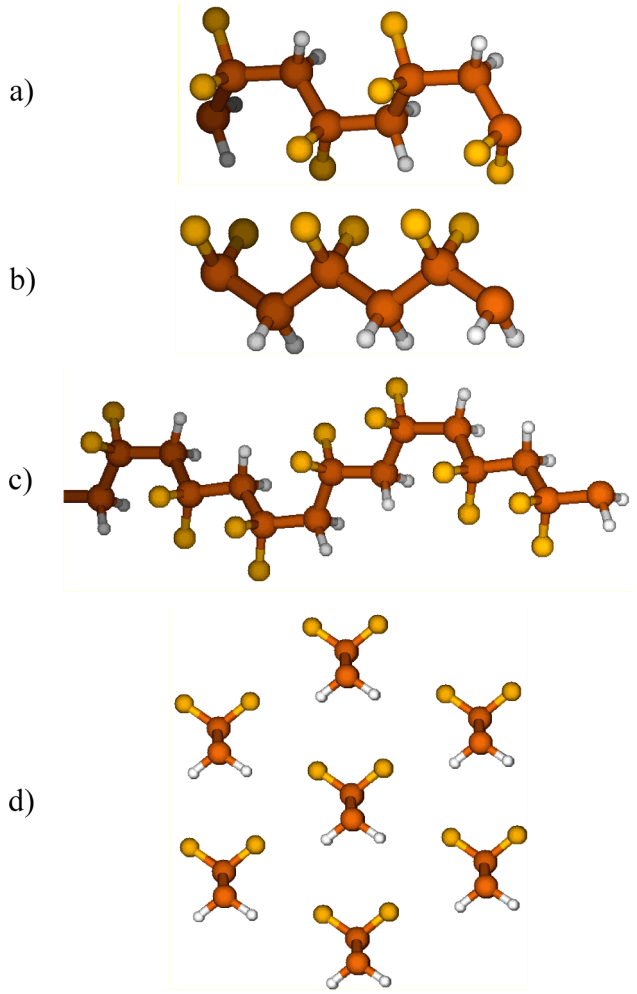

Figure 1. Sketches of different chains possessing, respectively, the conformation observed in (a) α- and δ-PVDF, (b) β-PVDF, and (c) γ-PVDF. In panel d, a sketch of the molecular packing observed in β-PVDF is provided.

DOI: 10.1021/acs.jpcb.5b00161
J. Phys. Chem. B 2015, 119, 4888−4897

Table 1. Comparison between DFT Computed Cell Parameters[a] of PVDF polymorphs

		B3LYP-D				PBE0-D				B3LYP		PBE0	
	expt	6-31G(d,p)	PE	pob-TZVP	PE	6-31G(d,p)	PE	pob-TZVP	PE	pob-TZVP	PE	pob-TZVP	PE
α form	*P21/c*												
a	4.96	4.752	*−4.2*	4.827	*−2.7*	4.744	*−4.4*	4.802	*−3.2*	5.056	*1.9*	5.025	*1.3*
b	9.64	8.980	*−6.8*	9.238	*−4.2*	8.925	*−7.4*	9.196	*−4.6*	9.846	*2.1*	9.725	*0.9*
c	4.62	4.651	*0.7*	4.650	*0.7*	4.624	*0.1*	4.617	*−0.1*	4.664	*0.9*	4.631	*0.2*
β	90	91.037	*1.2*	91.367	*1.5*	90.727	*0.8*	91.876	*2.1*	90.910	*1.0*	91.796	*2.0*
MPE			*−3.5*		*−2.1*		*−3.9*		*−2.6*		*1.7*		*0.8*
β form	*Cm2m*												
a	8.58	8.209	*−4.3*	8.369	*−2.5*	8.155	*−5.0*	8.297	*−3.3*	8.666	*1.0*	8.682	*1.2*
b	4.91	4.498	*−8.4*	4.597	*−6.4*	4.498	*−8.4*	4.568	*−7.0*	4.847	*−1.3*	4.770	*−2.8*
c	2.56	2.576	*0.6*	2.577	*0.6*	2.560	*−0.0*	2.561	*0.1*	2.579	*0.8*	2.565	*0.2*
MPE			*−4.0*		*−2.7*		*−4.5*		*−3.4*		*0.2*		*−0.5*
γ form	*Cc*												
a	4.96	4.750	*−4.2*	4.849	*−2.2*	4.726	*−4.7*	4.818	*−2.9*	5.040	*1.6*	5.008	*1.0*
b	9.67	9.063	*−6.3*	9.220	*−4.7*	9.064	*−6.3*	9.205	*−4.8*	9.745	*0.8*	9.683	*0.1*
c	9.2	9.219	*0.2*	9.259	*0.6*	9.149	*−0.6*	9.186	*−0.1*	9.301	*1.1*	9.226	*0.3*
β	93	99.788	*7.3*	99.383	*6.9*	99.323	*6.8*	99.310	*6.8*	94.506	*1.6*	95.571	*2.8*
MPE			*−3.4*		*−2.1*		*−3.8*		*−2.6*		*1.2*		*0.5*
δ form	*P21cn*												
a	4.62	4.649	*0.6*	4.654	*0.7*	4.619	*−0.0*	4.625	*0.1*	4.663	*0.9*	4.632	*0.3*
b	9.64	8.912	*−7.6*	9.141	*−5.2*	8.874	*−7.9*	9.070	*−5.9*	9.937	*3.1*	9.773	*1.4*
c	4.96	4.737	*−4.5*	4.813	*−3.0*	4.726	*−4.7*	4.793	*−3.4*	5.026	*1.3*	4.995	*0.7*
MPE			*−3.8*		*−3.2*		*−4.2*		*−3.1*		*1.8*		*0.8*

[a]Values of *a*, *b*, *c* parameters are in Å, and values of the angles are in degrees. B3LYP-D and PBE0-D refer to DFT calculations where Grimme correction for dispersion interaction (DFT-D) has been adopted. For each cell parameter, the percentage error (PE) with respect to the experimental datum has been calculated as (see Computational Details for references for the different experimental data): $PE = (PAR_{theo} - PAR_{exp}) \times 100/PAR_{exp}$, where PAR means the generic cell parameter (*a*, *b*, *c*, or β). Mean percentage errors (MPE) are also reported by averaging on the PE obtained for *a*, *b*, and *c* in each case

comparison, in order to take into account the implicit approximations adopted in the computational approach (i.e., neglect of anharmonicity, approximated treatment of electron correlation, finiteness of the basis sets, etc.), frequency scaling factors are introduced when comparing the DFT computed and experimental data: in this case, the calculated frequencies were scaled by 0.9594[57] (for the PBE0/pob-TZVP chosen for the prediction of the spectra, see next section) except in the figure showing the far-IR region below 600 cm^{-1} where the DFT spectra have been reported unscaled.

It should be noticed that our approach is not an "exact" description of the real systems: our calculations provide a reliable description of the crystal domains and of regular chain conformations (1D model chain) of polymers, but obviously they do not take into account the existence of the amorphous domains. Therefore, in the comparison with the experimental spectra or with other structural data, we need to consider that the real nature of semicrystalline polymers is only partially described by the computational approach here adopted since the features related to the amorphous contribution are obviously not reproduced by the calculation. Moreover, the geometry optimization does not take into account thermal effects or the presence of the other variables in a real environment. In any case, we will see that very good results are obtained concerning both the structural and spectroscopic properties, assessing the high reliability of the computational method adopted.

2.2. Experimental Details. The samples analyzed are Solef PVDF homopolymer produced by Solvay Specialty Polymers SpA in the form of powder/pellets or suitable preparation. Attenuated total reflectance (mid-infrared and far-infrared) spectra have been collected with a Thermo Nicolet 6700 FT-IR equipped with mid-infrared and far-infrared optics, with a variable temperature GladiATR Specac accessory: diamond crystal, single reflection, temperature range from RT to 190 °C, constant pressure during the temperature experiment given by the clamp of the accessory. All data provided have a spectral resolution of 2 cm^{-1}. Transmittance data to analyze the β-PVDF phase under pressure have been recorded with a Thermo Nicolet iS50 and a high pressure diamond cell (High Pressure Diamond Optics Inc.), mounted on 4× focusing optics (Spectra-Bench, Spectra-Tech, Inc..); the pressure reached is in the range of 10^2 kbar. FT-Raman spectra have been collected with a Thermo Nicolet Nexus 870 FT-IR instrument equipped with the Raman module, with a Nd:YAG laser (λ_{exc} = 1064 nm) and an InGaAs detector, power on the samples on the order of 10^2 mW, and 1024−4192 scans for a spectral resolution of 4 cm^{-1}. Solef PVDF 6008 homopolymer in powder form has been analyzed for RT and variable temperature (mid-IR and far-IR) measurements. Samples rich in β-PVDF have been obtained as follows: samples were cut according to 1A specimen shape described in ISO 527, both from extruded film made of Solef 1010 PVDF (100 μm thick) and from Solef 1012 PVDF compression molded plate having a thickness close to 1.5 mm. Afterward, specimens were stretched at 23 °C with a crosshead speed equal to 50 mm/min until they broke. IR and Raman analysis have been performed in the necked and yielded portion of the samples

3. RESULTS AND DISCUSSION

3.1. Crystal Structure and Conformation. The results of the full geometry and cell optimization of the four polymorphs

DOI: 10.1021/acs.jpcb.5b00161
J. Phys. Chem. B 2015, 119, 4888−4897

are reported in Table 1 for all the combinations of functional/basis sets adopted.

These results are quite significant and shed some new light on the computational method here adopted for the prediction of the structural properties of this system. Up to now, B3LYP-D/6-31G(d,p) calculations proved to be the best compromise for the prediction of the structural properties of polymer systems when suitable parameters for the Grimme correction are chosen.[43−47] Indeed, as expected, this correction proved to be required for a reliable description of the cell parameters related to intermolecular chain packing.

In the case of PVDF, a different behavior is observed for all four polymorphs: while the cell parameters related to chain repetition distance are very good in all cases (thus indicating a reliable description of the intramolecular structure of PVDF chains in the different polymorphs), large errors are predicted for the other two parameters, which are significantly underestimated. Original Grimme correction is known to overestimate the magnitude of dispersion interactions,[54−56] and in order to cure this deficiency, a suitable tuning of the parameters occurring in the correction and van der Waals radii in particular has been proposed.[43,54] However, this strategy seems to be not effective in the case of PVDF. Adopting the more extended pob-TZVP basis set, explicitly optimized for CRYSTAL calculations,[53] produces better agreement, consistent with the fact that an accurate description of intermolecular effects requires extended basis sets; however, the deviation with respect to the experimental data still remains quite large. In order to check also for possible effects due to DFT exchange-correlation functional, PBE0-D has been also adopted: a worse agreement is obtained with respect to B3LYP-D for both basis sets, thus indicating that the limitation of the current computational methods is not significantly dependent on the function or basis set choice.

In a very recent paper, Itoh et al.[35] carried out a computational investigation of PVDF polymorphs adopting the CRYSTAL code and found that the best method for the prediction of the structure of PVDF is indeed PBE0/TZVP without any correction for dispersion interaction. On this basis, we carried out B3LYP/pob-TZVP and PBE0/pob-TZVP without Grimme corrections, and we obtained a very good prediction of the crystal structure of all PVDF polymorphs. PBE0 in particular gave extremely good agreement with the experimental data, similar to the results reported in ref 35.

Not only is the discussion reported above important in the context of molecular modeling and first-principles calculations of polymers, but the results so obtained already give some indication on the molecular effects influencing the properties of PVDF. Indeed, the fact that the best agreement is obtained when no correction for dispersion interaction is introduced in the calculation reveals that the major contribution to intermolecular interaction is due to some other kind of force that is already well described by standard DFT. On these grounds, it is immediate to identify dipole−dipole interactions as the main responsible of chain packing in PVDF polymorphs. Their importance on the ferroelectric behavior of PVDF has been already pointed out in previous works,[31,32] and we will demonstrate in the next section how these interactions play a non-negligible role in affecting the vibrational properties of PVDF.

Considering the conformational properties of PVDF polymorphs, our calculations confirm the previous experimental and theoretical results: indeed, TGTG′, all-trans, and T_3GT_3G' conformations are predicted for α- (and δ-), β-, and γ-PVDF respectively.

In conclusion, the best computational methods proved to be PBE0/pob-TZVP; therefore, this combination has been used in the following for the discussion of the vibrational spectra and properties of PVDF.

3.2. IR and Raman Spectroscopy of PVDF Polymorphs. On the basis of the optimized crystal structures described in the previous section, we can now discuss the IR and Raman spectra predicted at PBE0/pob-TZVP level for the four different polymorphs of PVDF. Such a comparison is reported in Figure 2.

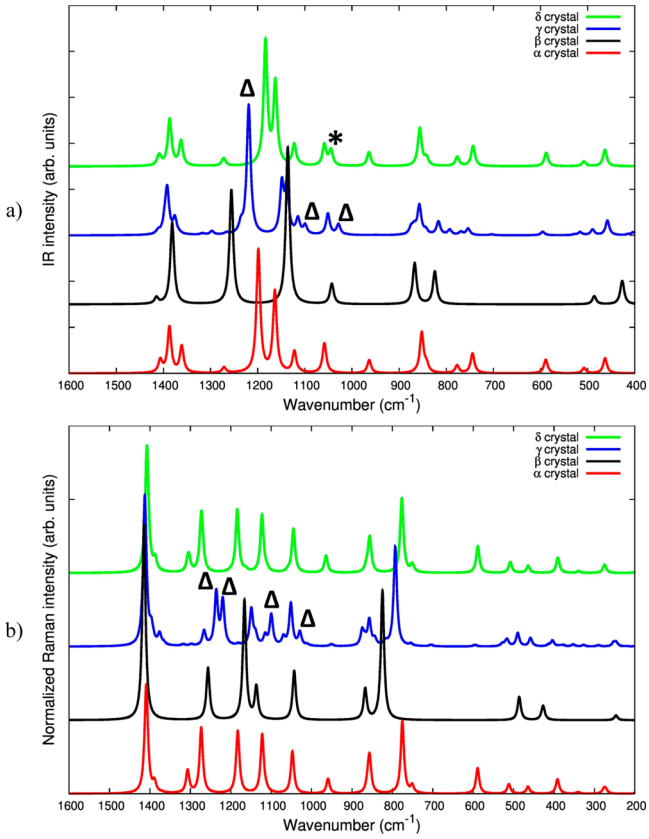

Figure 2. Comparison of the (a) IR and (b) Raman spectra of PVDF polymorphs as obtained by periodic DFT calculations (PBE0/pob-TZVP). All the spectra are scaled in frequency by 0.9594. Marker bands of γ and δ polymorphs are marked by △ and * respectively.

The DFT computed spectra reveal that PVDF polymorphs present peculiar spectral patterns, with well-defined markers bands that could be used for their identification; moreover they allow us to clearly discriminate among the different phases and can be also used for quantitative determination. The vibrational properties of the α and β phases will be described later also in relation to experimental measurements, and we will here comment more in detail on the vibrational properties of the elusive γ and δ polymorphs. Starting from the latter, whose structural properties have been revisited very recently,[15] we should recall that in this phase, the PVDF chains show the same conformation (TGTG′) observed in α form and also very similar cell parameters, thus indicating a similar molecular packing at the solid state. The main difference is indeed the relative orientation of the chains in the crystal, which, in the δ form, give rise to a net dipole moment per unit cell, responsible

DOI: 10.1021/acs.jpcb.5b00161
J. Phys. Chem. B 2015, 119, 4888−4897

for its ferroelectric response. These peculiarities justify also the fact that δ form has been also labeled as "polar α" in the past. Due to the strong similarities between α and δ concerning both their intramolecular and supramolecular structure, no significant differences are expected in the IR and Raman spectra: indeed, based on the comparison reported in Figure 2 and in Figure S1 of the Supporting Information, we can verify that the only difference in the spectral patterns could be found in the IR spectrum, where the δ form presents a doublet at about 1050 cm^{-1} (marked with * in Figure 2a) instead of the single band predicted and observed for the α phase. This minor difference would be further obscured by the fact that the above features fall in a spectral region where a broad contribution due to the amorphous phase is also present (see, for instance, spectrum of the melt in Figure 5), making this doublet not so easily observable. In the case of the Raman spectrum, these two polymorphs show spectra that are practically identical, thus excluding the possibility to adopt Raman spectroscopy for the characterization of δ phase. As a conclusion, we can state that vibrational spectroscopy is not able to identify the possible occurrence of a portion of δ crystal phase in a PVDF sample. Considering now γ phase, characterized by a chain conformation different from the α phase, we can verify that the situation is less difficult both in the IR and in particular in the Raman spectra. In the mid-IR, DFT calculations show that the main bands predicted for γ-PVDF are superimposed to bands due to either α- or β-PVDF but three possible marker bands are calculated at 1218, 1100, and 1029 cm^{-1} (marked with Δ in Figure 2). However, similarly to the case of δ-PVDF, these bands fall in the region where the broad band due to amorphous PVDF is present, thus making it quite difficult to detect such weak signals in the spectrum. The experimental IR spectrum of γ-PVDF shows indeed a close resemblance to that of the β phase, and this correspondence has been pointed out also by other authors,[17,20,24,58,59] and it is shown by the spectra reported by Kobayashi et al.[17] Therefore, it is not so easy to obtain well-defined marker bands of this polymorph in the mid-IR region. We will show in the next section that in the far-IR region, important marker bands of γ-PVDF can be indeed detected.

On the other hand, in the case of the Raman spectra, Figure 2b shows that γ-PVDF could present sufficiently distinct marker bands, in particular the doublet observed at about 1250 cm^{-1} and the band at about 1100 cm^{-1}. These markers bands could be more easily detectable with respect to those in the IR spectrum, but a detailed experimental investigation is necessary to verify the results obtained by DFT calculations.

Moving now to the detailed discussion of α- and β-PVDF, in Figure 3 the DFT computed IR/Raman spectra are compared with the experimental spectra of samples containing α or β or mixtures of the two phases.

For both polymorphs and for both IR and Raman spectra, we can verify that the agreement between DFT calculations and experimental spectra is extremely good in all major and minor details.

Starting from the analysis of the IR spectrum, we can confirm the assignments of the most important marker bands, which have been proposed in the literature: it is indeed easy to verify that the band observed at 1275 cm^{-1} is clearly a marker of the β phase, similarly to the doublet at 874–840 cm^{-1} and the band at 508 cm^{-1}. In the case of the α phase, the markers bands are found in the experimental spectra at 975, 870, 796–760, 613, 531, and 485 cm^{-1}. DFT computed spectra unambiguously

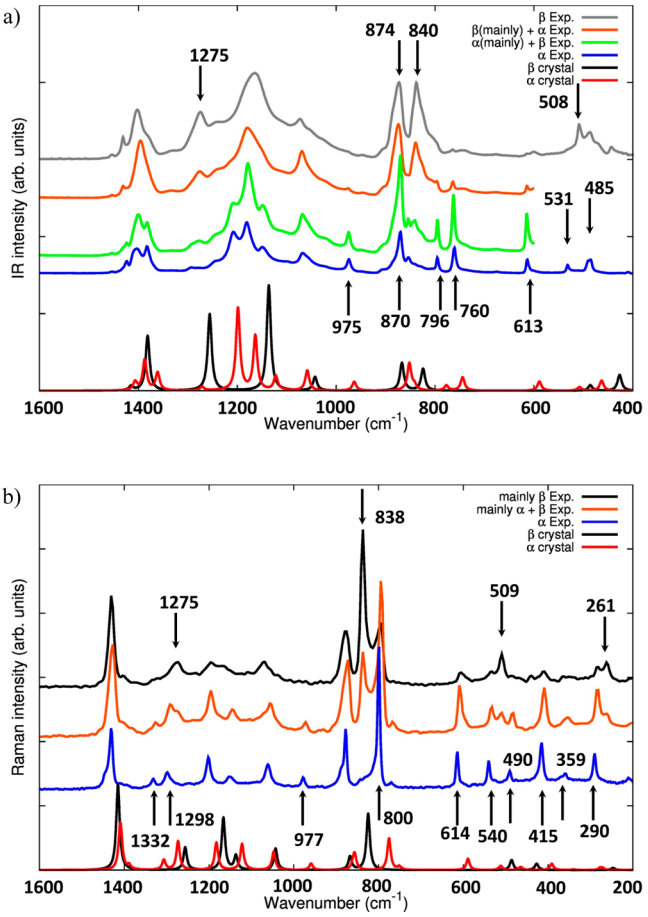

Figure 3. Comparison between experimental and DFT computed (PBE0/pob-TZVP) (a) IR and (b) Raman spectra of α-PVDF and β-PVDF. DFT computed spectra are scaled in frequency by 0.9594. Experimental spectra are reported for samples containing α-PVDF or β-PVDF or a mixture of the two phases. The most important marker bands for each polymorph are indicated (see also Table 2 and the Supporting Information). In Figure SI2 of the Supporting Information, we also reported the same comparison where the experimental IR spectra are reported after spectral subtraction of the amorphous contribution (spectrum of the melt, see Figure 5 and related discussion). No significant differences are observed, demonstrating the high crystallinity of the samples here analyzed.

confirm all these markers bands and their assignment to α or β phase, as clearly demonstrated by the comparison reported in Figure 3a. Furthermore, DFT computation allows us to explain the spectral pattern also in those regions that are hardly used for qualitative or quantitative evaluation of the content of the different phases in a given sample. Indeed, considering the group of bands just below 1400 cm^{-1}, the experimental spectrum of α phase shows three resolved bands, while only two are present for β-PVDF, as exactly predicted by the calculations. Furthermore, also the broad band at about 1200 cm^{-1} is more structured in α-PVDF, consistent with the results of the calculations. Therefore, we can conclude again that, in the case of PVDF, DFT calculations are extremely reliable in predicting the vibrational features of the different polymorphs. The validity of the assignments proposed can be further checked by considering the experimental IR spectra of samples containing also a small amount of α or β phases: in these cases indeed the appearance of weak signals due to the impurity exactly in correspondence of the marker bands of the less

DOI: 10.1021/acs.jpcb.5b00161
J. Phys. Chem. B 2015, 119, 4888–4897

abundant polymorph is a further confirmation of the effectiveness of these markers for identification.

Considering now the Raman spectra reported in Figure 3b, similar results are found: indeed DFT computed spectra are in excellent agreement with the experimental ones in all the details and allow us to identify the most important marker bands. In particular, in the case of β-PVDF marker bands are found at 261, 509, and 1275 cm^{-1} and the most important one at 838 cm^{-1}; on the other hand, marker bands of α-PVDF are found at 290, 359, 415, 490, 540, 614, 977, 1298, and 1332 cm^{-1} and the most important one at 800 cm^{-1}. All of them have a theoretical counterpart that can be identified unambiguously.

On these grounds, the analysis of the sample containing both α and β phases is particularly meaningful: the comparison with the spectrum of pure α-PVDF reveals the presence of a small amount of β-PVDF, which is indeed responsible for the occurrence of the signal at 838 cm^{-1}, of the middle band of the triplet at 509 cm^{-1}, and of the shoulder at 1275 cm^{-1}, thus providing a further confirmation of these assignments.

It should also be noted that the sample that is composed mainly of β phase presents intense signals at 800, 614, and 415 cm^{-1} due to the impurity of α phase, which is still present.

In Table 2, we report the summary of the most important IR and Raman marker bands identified for α- and β-PVDF, which

Table 2. List of DFT Computed (PBE0/pob-TZVP) and Experiment IR/Raman Marker Bands of α-PVDF and β-PVDF[a]

IR		Raman	
PBE0/pob-TZVP, unscaled [scaled (0.9594)]	expt	PBE0/pob-TZVP, unscaled [scaled (0.9594)]	expt
	α form		
482 [463]	485	408 [392]	415
614 [589]	613	484 [464]	490
776 [744]	760	533 [512]	540
810 [777]	796	614 [589]	614
888 [852]	870	808 [775]	800
1005 [964]	975	1000 [959]	977
		1327 [1273]	1298
		1362 [1307]	1332
	β form		
507 [486]	508	507 [486]	509
859 [824]	840	859 [824]	838
904 [867]	874	1309 [1256]	1275
1309 [1256]	1275		

[a]For each band, the sketch of the associated normal mode of vibration is reported in the Supporting Information. Frequency values scaled by 0.9594 are reported in brackets.

can be useful for qualitative and quantitative measurements in practical applications; in Table S9 of the Supporting Information, a sketch of the normal mode of vibration is reported for each of these bands.

Apart from the detailed assignment of the experimental spectra and the identification of the most important marker bands, DFT calculations are important to investigate the properties of these materials at a molecular and supramolecular scale.

As reported in the previous section, intermolecular interactions and dipole−dipole forces in particular are significant in PVDF. In order to further clarify their effects, we report in Figure 4 the comparison between DFT computed IR and Raman spectra of α and β crystal and single chains (1D crystals) possessing α and β conformations (TGTG′ and all-trans) respectively. In both cases, significant differences are observed between the 3D crystal and the single chain spectra, in both frequency and intensity pattern. These differences indicate that packing interactions are able to modulate significantly the intramolecular structure of PVDF chains both in terms of vibrational dynamics (i.e., changes in the force constants and thus frequency values) and also regarding the electrical properties (i.e., change in the dipole moment and polarizability derivatives and thus in IR and Raman intensities).

This finding has two important consequences in the description of the physics of PVDF polymorphs and related systems (co- and terpolymers): (1) Dipole−dipole interactions can induce a modulation of the structural and electronic properties of PVDF, the latter in particular being crucial for the ferro- and piezoelectric properties of this systems. Also in previous computational work, Nakhmanson et al.[31,32] demonstrated that cooperative effects between interacting PVDF chains strongly modulate the molecular dipole moment, which changed from 2.1 D (normalized to the monomeric units) in the isolated chain to 3 D for PVDF chains packed in β phase. The computed spectra in Figure 4 further support the fact that intermolecular dipole−dipole interactions strongly modulate the properties of PVDF: on these grounds vibrational spectroscopy can be thus used also in a different perspective to characterize the intermolecular properties of new systems based on PVDF, where also supramolecular properties should be carefully tuned to optimize the ferroelectric response. (2) From the viewpoint of vibrational spectroscopy of polymers,[60,61] usually in the past the interpretation of the spectra of a solid state sample was carried out by adopting a single chain model. Indeed, with the exception of hydrogen-bonded polymers (e.g., nylons) where the significant modulation of frequencies and intensities due to strong intermolecular interaction has been well-recognized for decades,[62] in the other cases only intramolecular effects (e.g., different conformations, defects, etc.) were taken into account, overlooking chain−chain interactions, which were expected to play a minor role in the modulation of the spectral pattern. The present study clearly shows that a single infinite chain model is not adequate for the reliable interpretation of the spectra of crystalline polymer materials, where dipole−dipole interactions could play a relevant role.

This fact has important implications also in all investigations where a combined computational and experimental approach is adopted: indeed usually PVDF-based systems have been modeled by considering small, noninteracting molecular models (i.e., adopting the so-called *oligomer approach*). Our calculations points out that particular attention should be paid when adopting such an approach, since important effects could be lacking or could be different if the contribution of intermolecular interactions is turned off.

3.3. Temperature Dependence of IR Spectra. In order to study in more detail the structural transition occurring in PVDF, in Figure 5 the thermal behavior of the IR spectra of a sample of α-PVDF is reported, starting from room temperature, heating until melting, and cooling back to room temperature. The aim of this experiment is to monitor, based on the marker bands identified for PVDF polymorphs, the structural evolution of the system and the possible transitions induced by temperature. Indeed, it should be noted that for example the

DOI: 10.1021/acs.jpcb.5b00161
J. Phys. Chem. B 2015, 119, 4888−4897

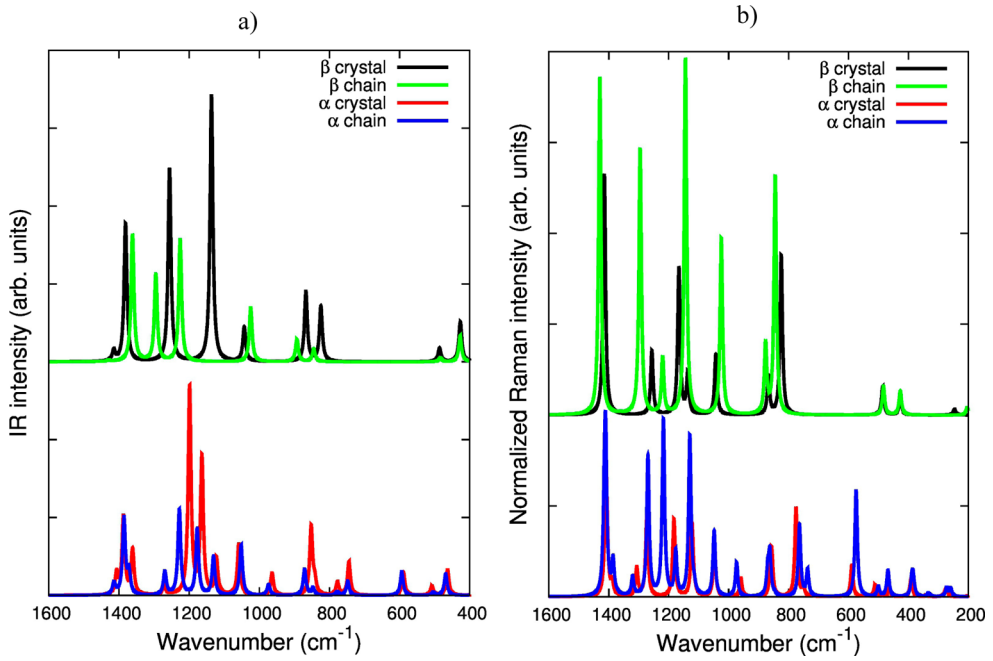

Figure 4. DFT computed (PBE0/pob-TZVP) (a) IR and (b) Raman spectra of α- and β-PVDF crystals compared with the spectra of the 1D infinite chains showing TGTG′ (α) and all-trans (β) conformations, respectively. All the spectra are scaled in frequency by a 0.9594 factor.

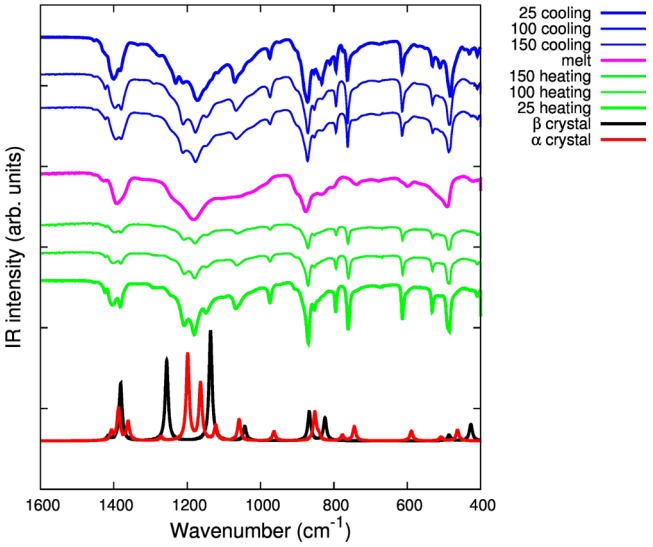

Figure 5. Evolution of the IR spectra of α-PVDF upon heating, melting, and cooling (as described in the Experimental Details section). The DFT computed spectra of α and β crystals (scaled by 0.9594) are also reported below.

γ phase can be generated by keeping the system at high temperatures in certain conditions.[11,14,20,59]

Starting from room temperature, it can be seen from the IR spectra that no transitions or defects are detectable since the spectra remain practically unaltered until melting. In other words, the α phase is stable, and no defects are generated before melting. The spectrum of the melt is reported in pink and shows the usual pattern with broad bands that is typical of a liquid or of an amorphous solid. Indeed, the spectrum of the melt often mimics quite well the spectrum of a hypothetically fully amorphous PVDF sample. Upon cooling back after melting, the markers bands of the α phase immediately reappear, thus indicating that recrystallization tends to return the overall system to the most stable α form. However, further weak bands appear, and in particular at room temperature, the markers bands of the β phase at 1275 cm^{-1}, the doublet at 874−840 cm^{-1}, and the band at 508 cm^{-1} are quite evident, thus apparently indicating that also a fraction of β phase is generated by cooling after melting (under pressure) in addition to the α form.

As a further analysis, in Figure 6, the thermal evolution of the spectra is followed also in the far-IR region of the spectrum below 600 cm^{-1}

Starting from the α-phase, we confirm that no transitions are observed until melting. Again, on cooling, the α form is mainly generated and in addition new bands are observed; in particular a new distinct band is observed at about 508 cm^{-1}, a doublet at 442−430 cm^{-1}, and two weak bands at 371 and 300 cm^{-1}.

The comparison with DFT computed spectra reveals that the band at 508 cm^{-1} can be indeed a marker of the β phase, as also confirmed by the spectrum of the sample containing a significant amount of this polymorph (gray spectrum); however, other new contributions are not all predicted for this polymorph. DFT calculations predicted for β-PVDF an intense band at about 450 cm^{-1}, which is indeed present in the experimental spectrum of β-PVDF and could be associated with the weak band appearing at 442 cm^{-1} after cooling (blue spectrum). However, the bands observed at 430 cm^{-1} and at 300 cm^{-1} cannot be associated either with α- or with β-PVDF based both on their experimental and the DFT computed spectra. Therefore, even if some of this evidence could support the growth of the β phase after the thermal treatment, some different structure should be taken into account to explain the appearance of all the different bands observed in the far-IR upon cooling. In this context DFT calculations give a fundamental contribution: in panel b of Figure 6, the comparison of DFT computed spectra of the α and γ crystal clearly demonstrates that the γ phase can explain all the new features observed upon cooling after melting under pressure of the clamp. Indeed, calculations on this polymorph show a

DOI: 10.1021/acs.jpcb.5b00161
J. Phys. Chem. B 2015, 119, 4888−4897

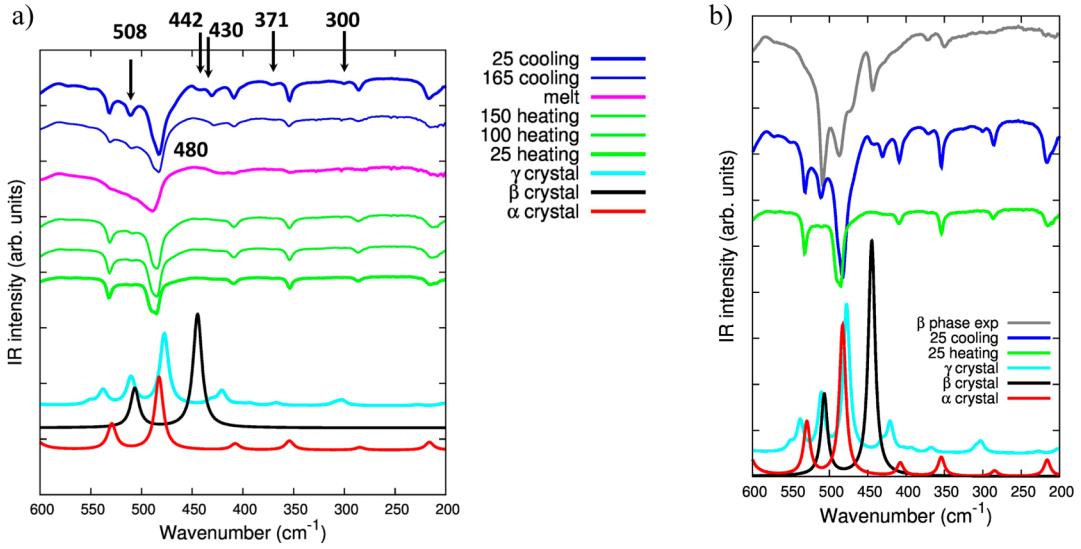

Figure 6. (a) Evolution of the far-IR spectra of α-PVDF upon heating, melting, and cooling (as described in the Experimental Details section). (b) Comparison between the far-IR spectra of α-PVDF (green), a sample with a significant amount of β-PVDF (gray), and the spectrum recorded at room temperature after heating, melting, and cooling (blue). The DFT computed spectra of α, β, and γ crystals (scaled by 0.9594) are also reported for a comparison in both panels.

marker band at 508 cm^{-1} similar to the β phase but also predict in the finest details the doublet at 442−430 cm^{-1} and the two weak bands at 371 and 300 cm^{-1}. Even the observed small downshift of the intense band at 480 cm^{-1} is predicted by the calculations. On the basis of the analysis reported, we can conclude that the far-IR suggests the formation of a very small amount of γ phase upon cooling after melting (under pressure). On the other hand, we previously showed that the new bands observed in the mid-IR (Figure 5) upon cooling indicate the generation of β phase. The above observations could seem partially contradictory, but they can be reconciled if we recall that γ phase shows mid-IR spectra very similar to that of the β phase (in particular both show the doublet at 870−840 cm^{-1} and the band at 1275 cm^{-1}), as pointed out by DFT calculations and by the experimental results.[16] Therefore, the spectrum observed in Figure 5 at room temperature after cooling cannot be necessarily taken as the evidence of the formation of a low amount of β phase, but it is also compatible with the formation of γ phase. This last interpretation would be now fully in agreement with the rationalization of far-IR data (Figure 6) given above.

This section has the following outcomes: on one hand, it shows that γ phase may be generated by very peculiar thermal and mechanical processes (while it has not been observed for other samples during severe working conditions). On the other hand, it demonstrates that this phase shows well-defined marker bands in the far-IR regions (doublet at 442−430 cm^{-1} and weak band at 300 cm^{-1}), which can be used for analytical purposes, as previously reported[19,63] mainly based on experimental data without quantum chemical modeling support.

4. CONCLUSIONS

In this work, the structural and the vibrational properties of PVDF polymorphs have been analyzed both experimentally and by means of state-of-the art periodic DFT calculations. Even if the vibrational properties of these systems have been widely investigated in the past also by means of first-principles approaches, a clear direct comparison between experimental and theoretical IR and Raman spectra has never been reported. Our calculations allowed us to give an interpretation in the finest detail of the experimental spectra, demonstrating how first-principles calculations nowadays can be a very powerful characterization tool in polymer science, which supports and completes the experimental observations. Furthermore, a combined experimental and computational study can give fundamental and useful indications for practical applications of vibrational spectroscopy in an industrial environment, as also demonstrated by a few other applications on fluorinated polymers previously presented by the authors.[64−67] Apart from the detailed interpretation of the spectra of α and β phase, our investigation gave new insights on the properties of the much more elusive γ phase and how the far-IR region of the spectrum can provide important information about this polymorph. This information is useful to tune polymer properties according to the final desired performances or applications. From the viewpoint of the molecular phenomena responsible for the structure−property relationship for PVDF-based polymers, we demonstrated that supramolecular dipole−dipole interactions are an essential ingredient for the interpretation of the vibrational spectra, and thus they will be absolutely not negligible when investigating the modulation of ferro- or piezoelectric properties of these systems. This finding is relevant not only for experimental and theoretical characterization but should be also taken into account in the study and optimization of new PVDF based systems displaying possibly interesting ferroelectric behavior.

■ ASSOCIATED CONTENT

Ⓢ Supporting Information

Figure with comparisons of experimental and DFT (PBE0/pob-TZVP) computed IR/Raman spectra of α- and δ-PVDF polymorphs, tables with DFT (PBE0/pob-TZVP) optimized values of the cell parameters and fractional atomic coordinates obtained by full optimization of the cell of crystals, tables with DFT (PBE0/pob-TZVP) computed values of frequencies, IR intensities, and normalized Raman intensities of PVDF polymorphs, sketches of the IR and Raman active modes

DOI: 10.1021/acs.jpcb.5b00161
J. Phys. Chem. B 2015, 119, 4888−4897

associated with the most significant marker bands of α-PVDF and β-PVDF crystals. This material is available free of charge via the Internet at http://pubs.acs.org.

AUTHOR INFORMATION

Corresponding Author

*Dr. Alberto Milani. E-mail: alberto.milani@polimi.it.

Notes

The authors declare no competing financial interest.

ACKNOWLEDGMENTS

S.R. gratefully acknowledges Giorgio Canil, Marco Mirenda, Giambattista Besana, and Flavio Tosi for preparing and providing suitable samples and for supporting the experimental work. Note: SOLEF is a registered trademark name of Solvay Specialty Polymers.

REFERENCES

(1) Kawai, H. The Piezoelectricity of Poly(vinylidene fluoride). *Jpn. J. Appl. Phys.* **1969**, *8*, 975−976.

(2) Lovinger, A. J. Ferroelectric Polymers. *Science* **1983**, *220*, 1115−1121.

(3) Furukawa, T.; Date, M.; Fukada, E.; Tajitsu, Y.; Chiba, A. Ferroelectric Behaviour in the Copolymer of Vinylidene Fluoride and Trifluoroethylene. *Jpn. J. Appl. Phys.* **1980**, *19*, L109−112.

(4) Furukawa, T. Ferroelectric Properties of Vinylidene Fluoride Copolymers. *Phase Transitions* **1989**, *18*, 143−211.

(5) Kochervinskii, V. V. Piezoelectricity in Crystallizing Ferroelectric Polymers: Poly(vinylidene fluoride) and its Copolymers (A Review). *Crystallogr. Rep.* **2003**, *48*, 649−675.

(6) Furukawa, T. Structure and Functional Properties of Ferroelectric Polymers. *Adv. Colloid Interface Sci.* **1997**, *71*−*72*, 183−208.

(7) Lang, S. B.; Muensit, S. Review of Some Lesser-known Applications of Piezoelectric and Pyroelectric Polymers. *Appl. Phys. A: Mater. Sci. Process.* **2006**, *85*, 125−134.

(8) Hasegawa, R.; Takahashi, Y.; Chatani, Y.; Tadokoro, H. Crystal Structures of Three Crystalline Forms of Poly(vinylidene fluoride). *Polym. J.* **1972**, *3*, 600−610.

(9) Hasegawa, R.; Kobayashi, M.; Tadokoro, H. Molecular Conformation and Packing of Poly(vinylidene fluoride). Stability of Three Crystalline Forms and the Effect of High Pressure. *Polym. J.* **1972**, *3*, 591−599.

(10) Bachmann, M. A.; Gordon, W. L.; Weinhold, S.; Lando, J. B. The Crystal Structure of Phase IV of Poly(vinylidene fluoride). *J. Appl. Phys.* **1980**, *51*, 5095−5099.

(11) Takahashi, Y.; Tadokoro, H. Crystal Structure of Form III of Poly(vinylidene fluoride). *Macromolecules* **1980**, *13*, 1317−1318.

(12) Takahashi, Y.; Matsubara, Y.; Tadokoro, H. Crystal Structure of Form II of Poly(vinylidene fluoride). *Macromolecules* **1983**, *16*, 1588−1592.

(13) Bachmann, M. A.; Lando, J. B. A Reexamination of the Crystal Structure of Phase II of Poly(vinylidene fluoride). *Macromolecules* **1981**, *14*, 40−46.

(14) Weinhold, S.; Litt, M. H.; Lando, J. B. The Crystal Structure of the γ Phase of Poly(vinylidene fluoride). *Macromolecules* **1980**, *13*, 1178−1183.

(15) Li, M.; Wondergem, H. J.; Spijkman, M. J.; Asadi, K.; Katsouras, I.; Blom, P. W. M.; de Leeuw, D. M. Revisiting the δ-phase of Poly(vinylidene fluoride) for Solution-Processed Ferroelectric Thin Films. *Nat. Mater.* **2013**, *12*, 433−438.

(16) Xia, F.; Cheng, Z.; Xu, H.; Li, H.; Zhang, Q.; Kavarnos, G. J.; Ting, R. Y.; Abdel-Sadek, G.; Belfield, K. D. High Electromechanical Responses in a Poly(vinylidene fluoride-trifluoroethylene-chlorofluoroethylene) Terpolymer. *Adv. Mater.* **2002**, *14*, 1574−1577.

(17) Kobayashi, M.; Tashiro, K.; Tadokoro, H. Molecular Vibrations of Three Crystal Forms of Poly(vinylidene fluoride). *Macromolecules* **1975**, *8*, 158−171.

(18) Cortili, G.; Zerbi, G. Chain Conformation of Polyvinylidene Fluoride as Derived from its Vibrational Spectrum. *Spectrochim. Acta A* **1967**, *23*, 285−299.

(19) Enomoto, S.; Kawai, Y.; Sugita, M. Infrared Spectrum of Poly(vinylidene fluoride). *J. Polym. Sci., Part A-2: Polym. Phys.* **1968**, *6*, 861−869.

(20) Benz, M.; Euler, W. B. Determination of the Crystalline Phases of Poly(vinylidene fluoride) Under Different Preparation Conditions Using Differential Scanning Calorimetry and Infrared Spectroscopy. *J. Appl. Polym. Sci.* **2003**, *89*, 1093−1100.

(21) Salimi, A.; Yousefi, A. A. FTIR Studies of β-phase Crystal Formation in Stretched PVDF Films. *Polym. Test.* **2003**, *22*, 699−704.

(22) Bachmann, M. A.; Koenig, J. L. Vibrational Analysis of Phase III of Poly(vinylidene fluoride). *J. Chem. Phys.* **1981**, *74*, 5896−5910.

(23) Bachmann, M. A.; Gordon, W. L.; Koenig, J. L.; Lando, J. B. An Infrared Study of Phase III Poly(vinylidene fluoride). *J. Appl. Phys.* **1979**, *50*, 6106−6112.

(24) Tashiro, K.; Kobayashi, M.; Tadokoro, H. Vibrational Spectra and Disorder-Order Transition of Poly(vinylidene fluoride) Form III. *Macromolecules* **1981**, *14*, 1757−1764.

(25) Ramer, N. J.; Raynor, C. M.; Stiso, K. A. Vibrational Frequency and LO−TO Splitting Determination for Planar−Zigzag β-poly-(vinylidene fluoride) Using Density-Functional Theory. *Polymer* **2006**, *47*, 424−428.

(26) Ramer, N. J.; Marrone, T.; Stiso, K. A. Structure and Vibrational Frequency Determination for α-Poly(vinylidene fluoride) Using Density-Functional Theory. *Polymer* **2006**, *47*, 7160−7165.

(27) Nakhmanson, S. M.; Korlacki, R.; Travis Johnston, J.; Ducharme, S.; Ge, Z.; Takacs, J. M. Vibrational Properties of Ferroelectric β-Vinylidene Fluoride Polymers and Oligomers. *Phys. Rev. B* **2010**, *81*, No. 174120.

(28) Ramer, N. J.; Stiso, K. A. Structure and Born Effective Charge Determination for Planar-Zigzag β-poly(vinylidene fluoride) Using Density Functional Theory. *Polymer* **2005**, *45*, 10431−10436.

(29) Wang, Z. Y.; Fan, H. Q.; Su, K. H.; Wen, Z. Y. Structure and Piezoelectric Properties of Poly(vinylidene fluoride) Studied by Density Functional Theory. *Polymer* **2006**, *47*, 7988−7996.

(30) Wang, W.; Fan, H.; Ye, Y. Effect of the Electric Field on the Structure and Piezoelectric Properties of Poly(vinylidene fluoride) Studied by Density Functional Theory. *Polymer* **2010**, *51*, 3575−3581.

(31) Nakhmanson, S. M.; Buongiorno Nardelli, M.; Bernholc, J. Collective Polarization Effects in β-polyvinylidene fluoride and its Copolymers with Tri- and Tetrafluoroethylene. *Phys. Rev. B* **2005**, *72*, No. 115210.

(32) Nakhmanson, S. M.; Buongiorno Nardelli, M.; Bernholc, J. Ab Initio Studied of Polarization and Piezoelectricity in Vinylidene Fluoride and BN-Based Polymers. *Phys. Rev. Lett.* **2004**, *92*, No. 115504.

(33) Duan, C. G.; Mei, W. N.; Yin, W. G.; Liu, J.; Hardy, J. R.; Ducharme, S.; Dowben, P. A. Simulations of Ferroelectric Polymer Film Polarization: The Role of Dipole Interactions. *Phys. Rev. B* **2004**, *69*, No. 235106.

(34) Su, H.; Strachan, A.; Goddard, W. A., III Density Functional Theory and Molecular Dynamics Studies of the Energetics and Kinetics of Electroactive Polymers: PVDDF and P(VDF-TrFE). *Phys. Rev. B* **2004**, *70*, No. 064101.

(35) Itoh, A.; Takahashi, Y.; Furukawa, T.; Yajima, H. Solid-state Calculations of Poly(vinylidene fluoride) Using the Hybrid DFT Method: Spontaneous Polarization of Polymorphs. *Polym. J.* **2014**, 1−5.

(36) Dovesi, R.; Orlando, R.; Erba, A.; Zicovich-Wilson, C. M.; Civalleri, B.; Casassa, S.; Maschio, M.; Ferrabone, M.; De La Pierre, M.; D'Arco, P.; et al. CRYSTAL14: A Program for the Ab Initio Investigation of Crystalline Solids. *Int. J. Quantum Chem.* **2014**, *114*, 1287−1317.

(37) Dovesi, R.; Saunders, V. R.; Roetti, C.; Orlando, R.; Zicovich-Wilson, C. M.; Pascale, F.; Civalleri, B.; Doll, K.; Harrison, N. M.; Bush, I. J.; D'Arco, P. et al. *CRYSTAL14 User's Manual*; University of Torino: Torino, IT, 2014.

DOI: 10.1021/acs.jpcb.5b00161
J. Phys. Chem. B 2015, 119, 4888−4897

(38) Maschio, L.; Kirtman, B.; Rérat, M.; Orlando, R.; Dovesi, R. Ab Initio Analytical Raman Intensities for Periodic Systems through a Coupled Perturbed Hartree-Fock/Kohn-Sham Method in an Atomic Orbital Basis. I. Theory. *J. Chem. Phys.* **2013**, *132*, No. 164101.
(39) Maschio, L.; Kirtman, B.; Rérat, M.; Orlando, R.; Dovesi, R. Ab Initio Analytical Raman Intensities for Periodic Systems through a Coupled Perturbed Hartree-Fock/Kohn-Sham Method in an Atomic Orbital Basis. II. Validation and Comparison with Experiments. *J. Chem. Phys.* **2013**, *132*, No. 164102.
(40) Torres, F. J.; Civalleri, B.; Meyer, A.; Musto, P.; Albunia, A. R.; Rizzo, P.; Guerra, G. Normal Vibrational Analysis of the Syndiotactic Polystyrene s(2/1)2 Helix. *J. Phys. Chem. B* **2009**, *113*, 5059−5071.
(41) Torres, F. J.; Civalleri, B.; Pisani, C.; Musto, P.; Albunia, A. R.; Guerra, G. Normal Vibrational Analysis of a trans-Planar Syndiotactic Polystyrene Chain. *J. Phys. Chem. B* **2007**, *111*, 6327−6335.
(42) Ferrari, A. M.; Civalleri, B.; Dovesi, R. Ab Initio Periodic Study of the Conformational Behavior of Glycine Helical Homopeptides. *J. Comput. Chem.* **2010**, *31*, 1777−1784.
(43) Quarti, C.; Milani, A.; Civalleri, B.; Orlando, R.; Castiglioni, C. Ab Initio Calculation of the Crystalline Structure and IR Spectrum of Polymers: Nylon 6 Polymorphs. *J. Phys. Chem. B* **2012**, *116*, 8299−8311.
(44) Galimberti, D.; Quarti, C.; Milani, A.; Brambilla, L.; Civalleri, B.; Castiglioni, C. IR Spectroscopy of Crystalline Polymers from Ab Initio Calculations: Nylon 6,6. *Vib. Spectrosc.* **2013**, *66*, 83−92.
(45) Quarti, C.; Milani, A.; Castiglioni, C. Ab Initio Calculation of the IR Spectrum of PTFE: Helical Symmetry and Defects. *J. Phys. Chem. B* **2013**, *117*, 706−718.
(46) Milani, A.; Galimberti, D. Polymorphism of Poly(butylene terephthalate) Investigated by Means of Periodic Density Functional Theory Calculations. *Macromolecules* **2014**, *47*, 1046−1052.
(47) Galimberti, D.; Milani, A. Crystal Structure and Vibrational Spectra of Poly(trimethylene terephthalate) from Periodic Density Functional Theory Calculations. *J. Phys. Chem. B* **2014**, *118*, 1954−1961.
(48) Milani, A. A Revisitation of the Polymorphism of Poly(butylene-2,6-naphthalate) from Periodic First-Principles Calculations. *Polymer* **2014**, *55*, 3729−3735.
(49) Milani, A. Unpolarized and Polarized Raman Spectroscopy of Nylon-6 Polymorphs: A Quantum Chemical Approach. *J. Phys. Chem. B* **2015**, *119*, 3868−3874.
(50) Becke, A. Density-Functional Thermochemistry. III. The Role of Exact Exchange. *J. Chem. Phys.* **1993**, *98*, 5648−5652.
(51) Lee, C.; Yang, W.; Parr, R. Development of the Colle-Salvetti Correlation-Energy Formula into a Functional of the Electron Density. *Phys. Rev. B* **1988**, *37*, 785−789.
(52) Adamo, C.; Barone, V. Toward Reliable Density Functional Methods without Adjustable Parameters: The PBE0Model. *J. Chem. Phys.* **1999**, *110*, 6158−6170.
(53) Peintinger, M. F.; Oliveira, D. V.; Bredow, T. Consistent Gaussian Basis Set of Triple-Zeta Valence with Polarization Quality for Solid-State Calculations. *J. Comput. Chem.* **2013**, *34*, 451−459.
(54) Civalleri, B.; Zicovich-Wilson, C. M.; Valenzano, L.; Ugliengo, P. B3LYP Augmented with an Empirical Dispersion Term (B3LYP-D*) as Applied to Molecular Crystals. *CrystEngComm* **2008**, *10*, 405−410.
(55) Grimme, S. Accurate Description of van der Waals Complexes by Density Functional Theory Including Empirical Corrections. *J. Comput. Chem.* **2004**, *25*, 1463−1473.
(56) Grimme, S. Semiempirical GGA-type Density Functional Constructed with a Long-Range Dispersion Correction. *J. Comput. Chem.* **2006**, *27*, 1787−1799.
(57) Merrick, J. P.; Moran, D.; Radom, L. An Evaluation of Harmonic Vibrational Frequency Scale Factors. *J. Phys. Chem. A* **2007**, *111*, 11683−11700.
(58) Reynolds, N. M.; Kim, K. J.; Chang, C.; Hsu, S. L. Spectroscopic Analysis of Electric Field Induced Structural Changes in Vinylidene Fluoride/Trifluoroethylene Copolymers. *Macromolecules* **1989**, *22*, 1092−1100.
(59) Imamura, R.; Silva, A. B.; Gregorio, R. $\gamma \rightarrow \beta$ Phase Transformation Induced in Poly(vinylidene fluoride) by Stretching. *J. Appl. Polym. Sci.* **2008**, *110*, 3242−3246.
(60) Painter, P. C.; Coleman, M. M.; Koening, J. L. *The Theory of Vibrational Spectroscopy and its Application to Polymeric Materials*; Wiley: Chichester. 1982.
(61) Zbinden, R. *Infrared Spectroscopy of High Polymers*; Academic Press: New York, 1964.
(62) Pimentel, G. C.; McClellan, A. L. *The Hydrogen Bond*; W.H. Freeman: San Francisco, 1960.
(63) Gregorio, R., Jr. Determination of the α, β and γ Crystaline Phases of Poly(vinylidene fluoride) Films Prepared at Different Conditions. *J. Appl. Polym. Sci.* **2006**, *100*, 3272−3279.
(64) Milani, A.; Castiglioni, C.; Di Dedda, E.; Radice, S.; Canil, G.; Di Meo, A.; Picozzi, R.; Tonelli, C. Hydrogen Bonding Effects in Perfluorinated Polyamides: An Investigation Based on Infrared Spectroscopy and Density Functional Theory Calculations. *Polymer* **2010**, *51*, 2597−2610.
(65) Milani, A.; Tommasini, M.; Castiglioni, C.; Zerbi, G.; Radice, S.; Canil, G.; Toniolo, P.; Triulzi, F.; Colaianna, P. Spectroscopic Studies and First-Principles Modelling of 2,2,4-trifluoro-5-trifluoromethoxy-1,3-dioxole (TTD) and TTD−TFE Copolymers (Hyflon® AD). *Polymer* **2008**, *49*, 1812−1822.
(66) Radice, S.; Di Dedda, E.; Tonelli, C.; Della Pergola, R.; Milani, A.; Castiglioni, C. FT-IR Spectroscopy and DFT Calculations on Fluorinated Macromer Diols: IR Intensity and Association Properties. *J. Phys. Chem. B* **2010**, *114*, 6332−6336.
(67) Milani, A.; Zanetti, J.; Castiglioni, C.; Di Dedda, E.; Radice, S.; Canil, G.; Tonelli, C. Intramolecular and Intermolecular OH···O and OH···F Interactions in Perfluoropolyethers with Polar End Groups: IR Spectroscopy and First-Principles Calculations. *Eur. Polym. J.* **2012**, *48*, 391−403.

DOI: 10.1021/acs.jpcb.5b00161
J. Phys. Chem. B 2015, 119, 4888−4897